

Supplement: Zircon luminescence dating revisited

Christoph Schmidt¹, Théo Halter¹, Paul R. Hanson², Alexey Ulianov³, Benita Putlitz³, Georgina E. King¹, Sebastian Kreutzer⁴

¹Institute of Earth Surface Dynamics, University of Lausanne, Lausanne, 1015, Switzerland

²School of Natural Resources, University of Lincoln-Nebraska, Lincoln, 68583, United States of America

³Institute of Earth Sciences, University of Lausanne, Lausanne, 1015, Switzerland

⁴Institute of Geography, Heidelberg University, 69120 Heidelberg, Germany

Correspondence to: Christoph Schmidt (christoph.schmidt@unil.ch)

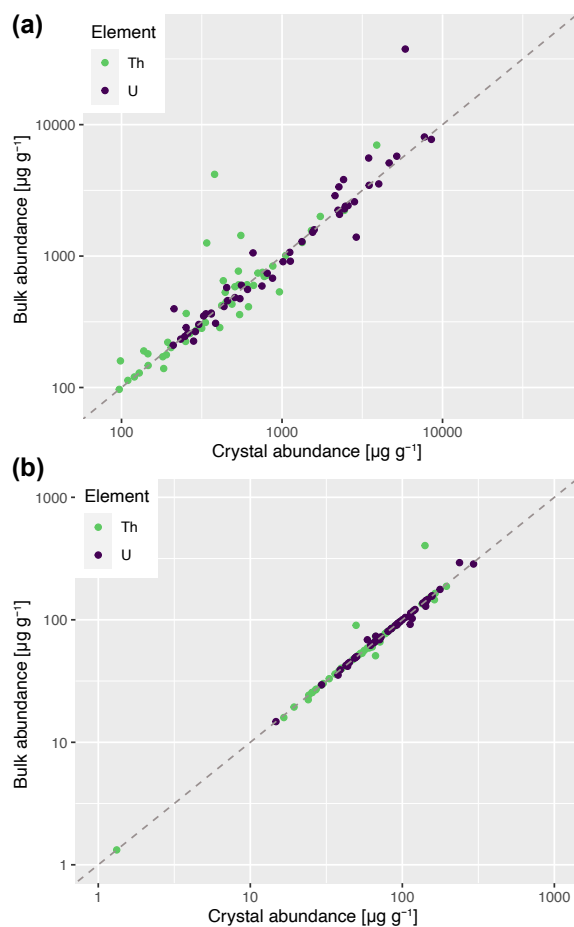


Figure S1. Comparison of Th and U contents determined by signal integration of the entire transient ablation signal, including inclusions and impurities (bulk), or the signal component related to the ‘pure’ zircon crystal structure (crystal) for samples ZR229 (a) and Can1 (b). The dashed line represents the 1:1 line.

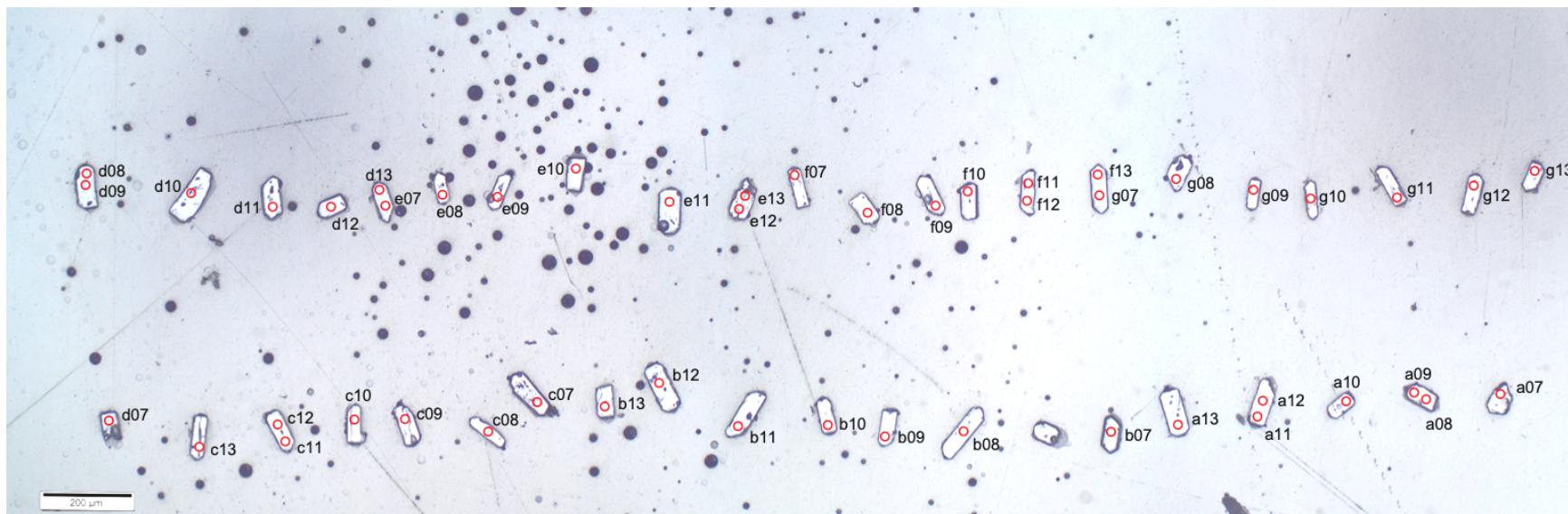


Figure S2. Scan of the mount with sample ZR229 with analytical spots indicated as red circles.

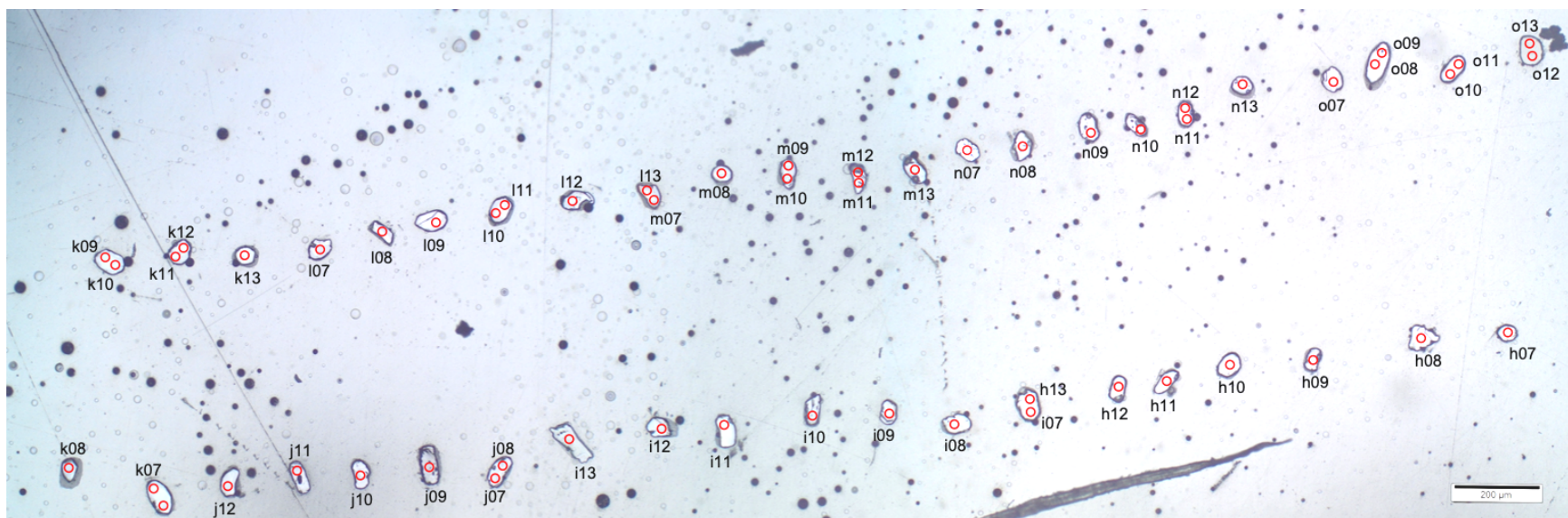
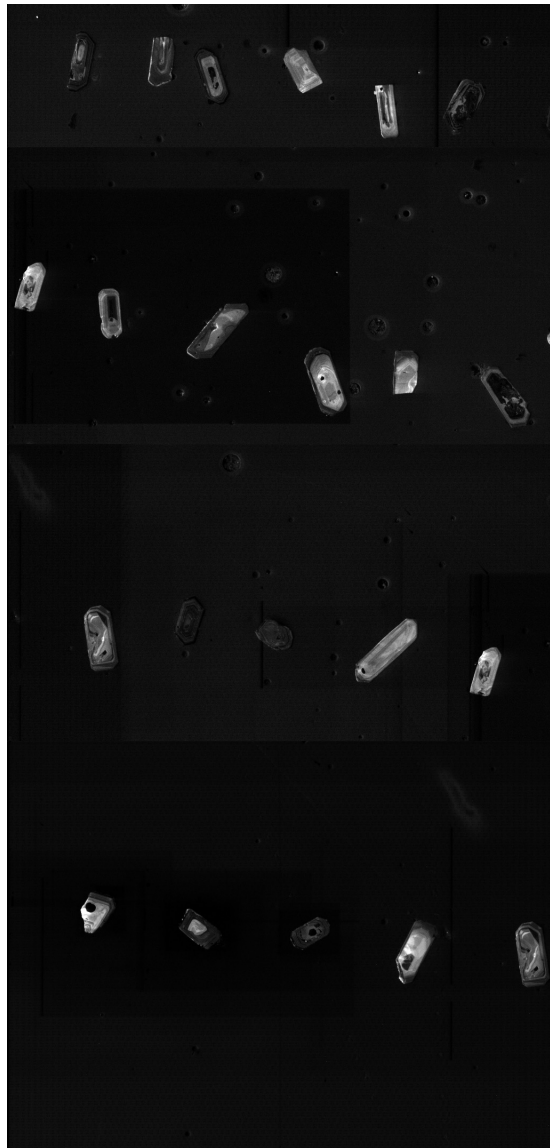
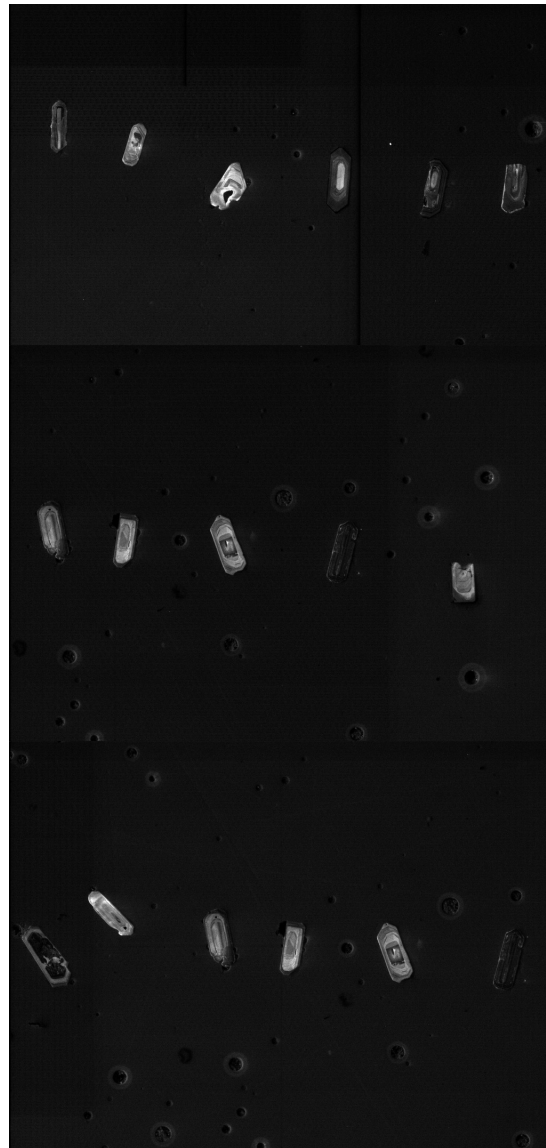


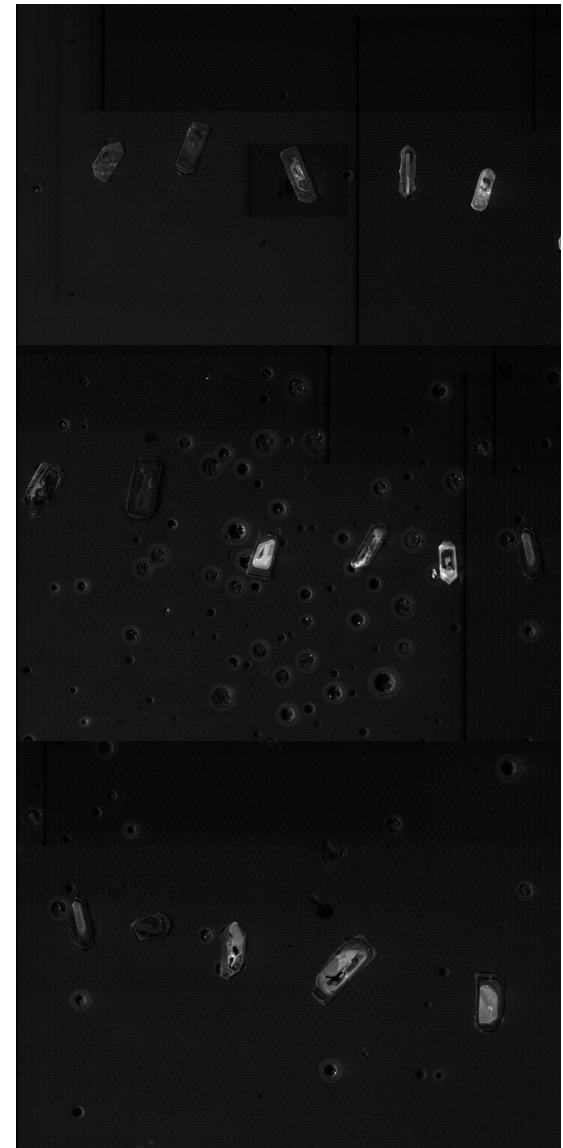
Figure S3. Scan of the mount with sample Can1 with analytical spots indicated as red circles.



SEM MAG: 182 x DET: KL
HV: 10.0 kV DATE: 08/11/23
VAC: HiVac Device: MV2300VP
500 um Vega @Tescan
SEM Geosciences Uni Lausanne



SEM MAG: 182 x DET: KL
HV: 10.0 kV DATE: 08/11/23
VAC: HiVac Device: MV2300VP
500 um Vega @Tescan
SEM Geosciences Uni Lausanne



SEM MAG: 182 x DET: KL
HV: 10.0 kV DATE: 08/11/23
VAC: HiVac Device: MV2300VP
500 um Vega @Tescan
SEM Geosciences Uni Lausanne

Figure S4. Cathodoluminescence images of the zircon sample ZR229.

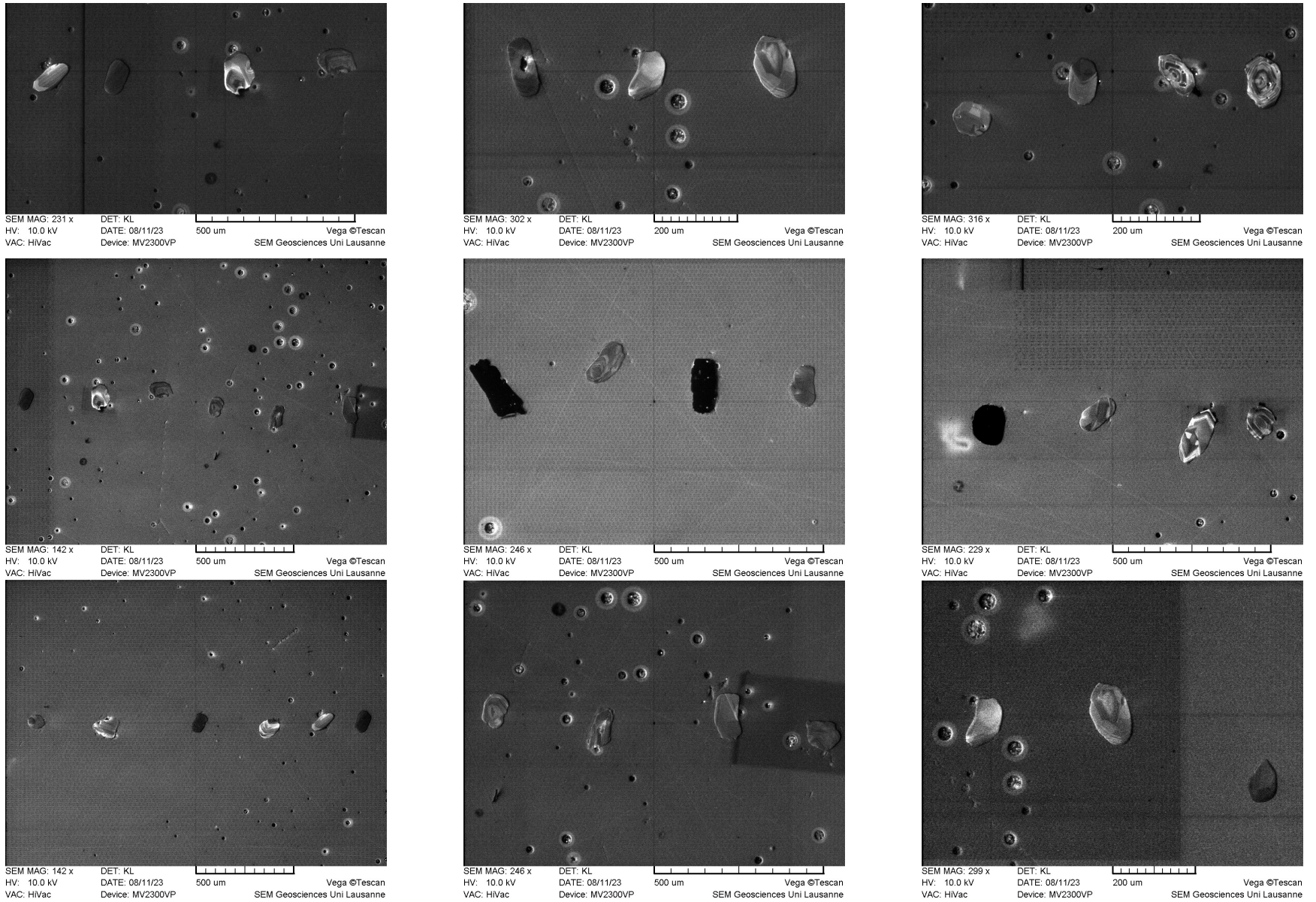
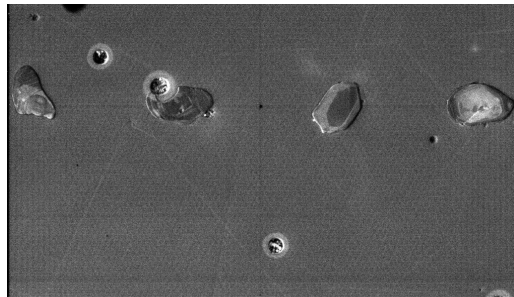
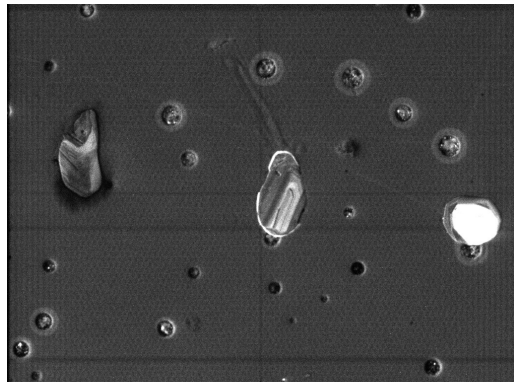


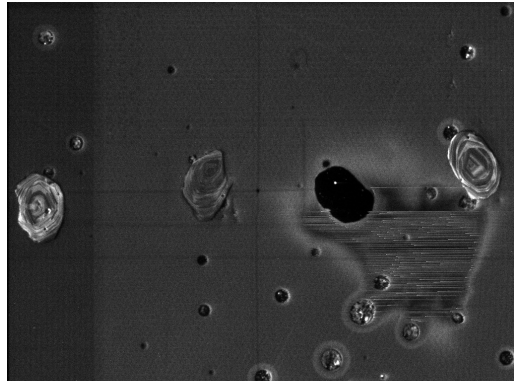
Figure S5. Cathodoluminescence images of the zircon sample Can1.



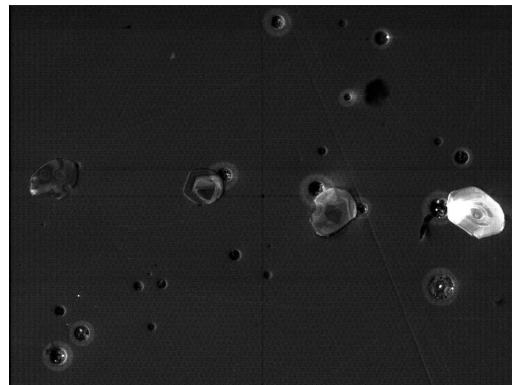
SEM MAG: 262 x DET: KL
HV: 10.0 kV DATE: 08/11/23 Vega ©Tescan
VAC: HiVac Device: MV2300VP SEM Geosciences Uni Lausanne



SEM MAG: 374 x DET: KL
HV: 10.0 kV DATE: 08/11/23 Vega ©Tescan
VAC: HiVac Device: MV2300VP SEM Geosciences Uni Lausanne



SEM MAG: 316 x DET: KL
HV: 10.0 kV DATE: 08/11/23 Vega ©Tescan
VAC: HiVac Device: MV2300VP SEM Geosciences Uni Lausanne



SEM MAG: 256 x DET: KL
HV: 10.0 kV DATE: 08/11/23 Vega ©Tescan
VAC: HiVac Device: MV2300VP SEM Geosciences Uni Lausanne

Figure S6. Cathodoluminescence images of the zircon sample Can1.

Table S5. Results of OSL decay curve decomposition into up to three components. For further details, see main text.

ZR229			ZR229-PH			Can1					
Hole #	Comp. 1 [cm ²]	Comp. 2 [cm ²]	Comp. 3 [cm ²]	Hole #	Comp. 1 [cm ²]	Comp. 2 [cm ²]	Comp. 3 [cm ²]	Hole #	Comp. 1 [cm ²]	Comp. 2 [cm ²]	Comp. 3 [cm ²]
1	3.19E-19	1.23E-21	NA	1	NA	NA	NA	1	1.25E-19	8.01E-21	NA
2	7.86E-21	NA	NA	2	1.58E-19	7.15E-21	NA	2	1.68E-19	NA	NA
3	6.64E-20	2.64E-21	NA	3	4.58E-21	NA	NA	3	1.24E-19	2.55E-21	NA
4	2.96E-19	1.77E-21	NA	4	1.96E-19	5.40E-20	6.20E-21	4	6.70E-20	3.67E-21	NA
5	NA	NA	NA	5	8.90E-20	8.93E-21	NA	5	8.37E-20	1.59E-21	NA
6	1.32E-19	1.36E-21	NA	6	9.85E-21	NA	NA	6	3.19E-21	NA	NA
7	NA	NA	NA	7	1.70E-19	4.87E-21	NA	7	2.48E-19	5.84E-21	NA
8	5.24E-22	NA	NA	8	2.74E-20	NA	NA	8	1.70E-19	6.39E-21	NA
9	1.72E-19	5.68E-21	NA	9	2.14E-19	7.15E-21	NA	9	1.46E-19	3.32E-21	NA
10	1.15E-21	NA	NA	10	1.00E-19	4.75E-21	NA	10	9.93E-20	2.05E-21	NA
11	1.77E-19	3.88E-21	NA	11	6.98E-21	NA	NA	11	2.40E-22	NA	NA
12	1.64E-19	7.52E-21	NA	12	1.12E-19	1.16E-20	NA	12	9.19E-21	NA	NA
13	2.65E-19	4.75E-20	3.53E-21	13	1.18E-20	NA	NA	13	5.86E-21	NA	NA
14	9.82E-20	2.43E-21	NA	14	1.88E-19	9.15E-21	NA	14	1.98E-19	1.10E-20	NA
15	2.63E-19	8.42E-21	NA	15	1.95E-19	5.75E-21	NA	15	4.84E-21	NA	NA
16	1.38E-19	6.84E-21	NA	16	1.40E-19	1.06E-20	NA	16	1.80E-19	1.05E-20	NA
17	9.80E-20	3.94E-21	NA	17	1.20E-19	4.17E-21	NA	17	1.27E-19	1.07E-20	NA
18	1.45E-19	3.73E-21	NA	18	7.94E-20	1.35E-21	NA	18	2.44E-19	2.52E-20	1.31E-21
19	6.57E-21	NA	NA	19	3.00E-20	7.14E-21	NA	19	1.97E-19	4.57E-21	NA
20	6.29E-21	NA	NA	20	1.47E-19	7.81E-21	NA	20	5.19E-20	5.06E-22	NA
21	8.55E-20	NA	NA	21	NA	NA	NA	21	4.12E-21	NA	NA
22	5.24E-21	NA	NA	22	7.26E-20	NA	NA	22	1.02E-19	5.11E-21	NA
23	1.20E-19	1.51E-21	NA	23	1.51E-19	6.10E-21	NA	23	7.09E-20	2.02E-20	3.68E-21
24	2.17E-19	1.69E-21	NA	24	8.77E-20	4.88E-21	NA	24	1.05E-19	5.23E-21	NA
25	1.74E-19	4.12E-21	NA	25	2.06E-19	1.03E-20	NA	25	2.37E-19	1.14E-20	NA
26	1.17E-19	2.29E-21	NA	26	2.29E-19	9.26E-21	NA	26	1.48E-19	5.61E-21	NA
27	1.62E-19	3.68E-21	NA	27	9.28E-20	NA	NA	27	1.28E-19	6.83E-21	NA
28	1.64E-19	4.42E-21	NA	28	1.26E-19	4.77E-21	NA	28	1.57E-19	9.07E-21	NA
29	2.61E-21	NA	NA	29	3.66E-21	NA	NA	29	1.28E-19	4.45E-21	NA
30	NA	NA	NA	30	1.31E-19	7.45E-21	NA	30	2.86E-19	5.94E-21	NA
31	2.19E-19	4.90E-21	NA	31	1.46E-19	8.93E-21	NA	31	4.47E-20	NA	NA
32	1.59E-19	2.41E-21	NA	32	3.71E-20	NA	NA	32	1.30E-20	NA	NA
33	1.91E-19	2.10E-21	NA	33	1.58E-19	1.11E-20	NA	33	1.89E-19	4.13E-20	4.63E-21
34	1.77E-20	NA	NA	34	2.95E-20	NA	NA	34	6.75E-20	4.50E-21	NA
35	2.42E-19	5.13E-20	5.47E-21	35	1.93E-19	1.11E-20	NA	35	3.12E-21	NA	NA
36	NA	NA	NA	36	9.85E-20	5.65E-21	NA	36	2.05E-19	3.30E-20	1.31E-21
37	2.49E-19	NA	NA	37	6.40E-20	8.19E-21	NA	37	2.60E-20	2.50E-21	NA
38	1.84E-19	5.97E-21	NA	38	4.59E-22	NA	NA	38	3.28E-20	NA	NA
39	1.37E-19	2.38E-21	NA	39	3.72E-21	NA	NA	39	1.58E-19	1.98E-20	1.80E-21
40	1.32E-21	NA	NA	40	1.62E-19	3.32E-20	6.09E-21	40	2.50E-19	9.89E-21	NA
41	1.19E-19	NA	NA	41	1.22E-21	NA	NA	41	1.54E-19	1.29E-20	7.70E-22
42	1.40E-19	4.15E-20	6.80E-21	42	2.11E-19	7.35E-21	NA	42	1.07E-19	5.68E-21	NA
43	1.65E-19	4.03E-21	NA	43	2.29E-19	1.38E-20	NA	43	1.56E-19	2.73E-21	NA
44	9.30E-20	5.53E-21	NA	44	2.11E-19	1.21E-20	NA	44	2.28E-19	4.25E-21	NA
45	5.89E-20	NA	NA	45	2.56E-20	6.76E-21	NA	45	1.14E-19	8.95E-21	NA
46	2.61E-19	9.99E-21	NA	46	1.48E-19	6.60E-21	NA	46	1.07E-19	6.77E-21	NA
47	1.76E-19	1.97E-21	NA	47	9.86E-20	5.14E-21	NA	47	3.15E-21	NA	NA
48	1.66E-19	4.38E-21	NA	48	6.37E-21	NA	NA	48	3.83E-20	NA	NA
49	1.69E-19	1.19E-20	NA	49	2.31E-19	7.08E-21	NA	49	7.96E-20	1.58E-21	NA
50	1.57E-19	4.58E-21	NA	50	1.67E-19	7.29E-21	NA	50	8.37E-20	3.95E-21	NA
51	1.60E-19	8.02E-21	NA	51	1.53E-19	8.62E-21	NA	51	1.47E-19	3.34E-21	NA
52	2.98E-20	NA	NA	52	1.32E-19	5.51E-21	NA	52	2.59E-19	2.11E-21	NA
53	2.87E-19	8.12E-21	NA	53	6.30E-21	NA	NA	53	1.08E-19	2.32E-20	2.38E-21
54	1.39E-19	3.44E-21	NA	54	2.12E-19	4.18E-20	6.04E-21	54	1.18E-19	6.83E-21	NA
55	4.48E-20	NA	NA	55	9.09E-20	6.99E-21	NA	55	7.64E-20	4.82E-21	NA
56	2.83E-20	NA	NA	56	8.14E-20	1.78E-21	NA	56	2.20E-19	3.23E-20	1.68E-21
57	5.50E-20	NA	NA	57	1.14E-19	4.74E-21	NA	57	5.95E-20	2.69E-21	NA
58	1.41E-19	4.25E-21	NA	58	8.52E-21	NA	NA	58	6.65E-20	5.57E-21	NA
59	2.96E-21	NA	NA	59	5.83E-20	NA	NA	59	2.81E-20	NA	NA
60	NA	NA	NA	60	3.00E-19	1.25E-20	NA	60	2.73E-20	2.63E-21	NA
61	1.44E-19	2.19E-21	NA	61	5.29E-21	NA	NA	61	3.72E-21	NA	NA
62	NA	NA	NA	62	1.78E-20	NA	NA	62	1.24E-19	2.77E-20	5.21E-21
63	1.24E-19	4.27E-21	NA	63	1.78E-19	1.73E-20	2.82E-21	63	2.49E-19	4.06E-20	3.63E-21
64	5.18E-20	NA	NA	64	5.18E-20	3.37E-21	NA	64	3.88E-21	NA	NA
65	2.84E-19	4.82E-20	4.42E-21	65	2.69E-19	8.01E-21	NA	65	4.72E-20	1.36E-21	NA
66	2.07E-19	3.30E-21	NA	66	6.15E-20	5.14E-21	NA	66	2.16E-19	1.34E-20	NA
67	1.34E-19	5.17E-21	NA	67	2.05E-19	4.50E-21	NA	67	9.75E-20	6.75E-21	NA
68	6.22E-20	NA	NA	68	8.08E-20	7.35E-21	NA	68	1.32E-19	3.02E-21	NA
69	4.39E-20	NA	NA	69	1.87E-19	6.49E-21	NA	69	1.00E-19	4.44E-21	NA
70	1.72E-19	7.93E-21	NA	70	1.79E-19	3.08E-20	4.19E-21	70	1.76E-19	9.38E-21	NA
71	2.14E-19	7.73E-21	NA	71	1.43E-19	6.17E-21	NA	71	3.06E-20	NA	NA

72	1.91E-19	6.80E-21	NA	72	2.50E-20	NA	NA	72	1.15E-20	NA	NA
73	6.19E-20	NA	NA	73	1.64E-19	3.26E-20	6.42E-21	73	2.22E-19	5.70E-21	NA
74	1.46E-19	6.03E-21	NA	74	1.54E-19	8.61E-21	NA	74	1.68E-19	2.73E-20	3.59E-21
75	8.32E-20	3.44E-21	NA	75	6.25E-21	NA	NA	75	7.90E-20	6.14E-21	NA
76	1.56E-19	5.70E-21	NA	76	1.56E-19	1.05E-20	NA	76	1.49E-19	5.27E-21	NA
77	5.94E-21	NA	NA	77	8.72E-20	6.48E-21	NA	77	1.75E-19	1.22E-20	NA
78	2.49E-19	4.93E-21	NA	78	4.97E-21	NA	NA	78	9.61E-20	1.01E-20	NA
79	8.47E-20	3.50E-21	NA	79	1.65E-20	NA	NA	79	2.81E-19	4.79E-21	NA
80	1.78E-19	5.93E-21	NA	80	1.68E-19	4.73E-21	NA	80	6.92E-20	NA	NA
81	2.84E-21	NA	NA	81	1.54E-19	5.60E-21	NA	81	1.11E-19	2.54E-20	1.60E-21
82	1.94E-19	1.27E-20	NA	82	1.83E-21	NA	NA	82	1.31E-19	2.17E-21	NA
83	2.33E-19	1.20E-20	NA	83	2.25E-20	NA	NA	83	2.63E-19	4.88E-21	NA
84	1.49E-19	7.30E-21	NA	84	1.49E-19	8.68E-21	NA	84	8.27E-20	3.49E-21	NA
85	1.93E-19	6.70E-21	NA	85	1.26E-19	7.74E-21	NA	85	7.42E-20	1.76E-21	NA
86	2.30E-19	9.70E-21	NA	86	8.79E-20	NA	NA	86	2.15E-20	NA	NA
87	9.79E-20	5.43E-21	NA	87	NA	NA	NA	87	2.92E-21	NA	NA
88	2.71E-19	3.70E-20	4.82E-21	88	9.41E-20	1.93E-21	NA	88	1.19E-19	2.31E-21	NA
89	3.78E-20	NA	NA	89	1.37E-19	1.02E-20	NA	89	1.14E-20	NA	NA
90	1.08E-19	4.36E-21	NA	90	7.11E-20	NA	NA	90	6.68E-21	NA	NA
91	1.43E-19	4.13E-21	NA	91	7.34E-21	NA	NA	91	5.22E-20	NA	NA
92	1.05E-19	1.71E-21	NA	92	3.04E-20	NA	NA	92	2.02E-19	5.98E-21	NA
93	1.57E-19	7.97E-21	NA	93	3.69E-20	NA	NA	93	6.33E-20	6.68E-21	NA
94	1.82E-19	3.84E-21	NA	94	3.00E-20	NA	NA	94	5.36E-20	NA	NA
95	9.09E-20	NA	NA	95	2.16E-19	2.59E-20	3.46E-21	95	1.35E-19	3.56E-20	4.87E-21
96	2.73E-19	3.32E-21	NA	96	1.32E-19	3.97E-21	NA	96	1.08E-19	6.87E-21	NA
97	1.20E-19	7.15E-21	NA	97	2.11E-19	5.59E-21	NA	97	3.66E-20	2.39E-21	NA
98	8.27E-20	NA	NA	98	1.94E-20	NA	NA	98	2.50E-19	1.31E-20	NA
99	2.09E-19	3.52E-20	2.39E-21	99	1.37E-19	8.29E-21	NA	99	1.72E-19	1.14E-20	NA
100	NA	NA	NA	100	3.49E-20	NA	NA	100	9.67E-20	7.63E-21	NA

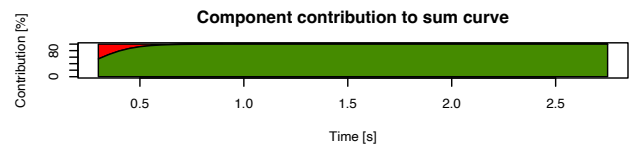
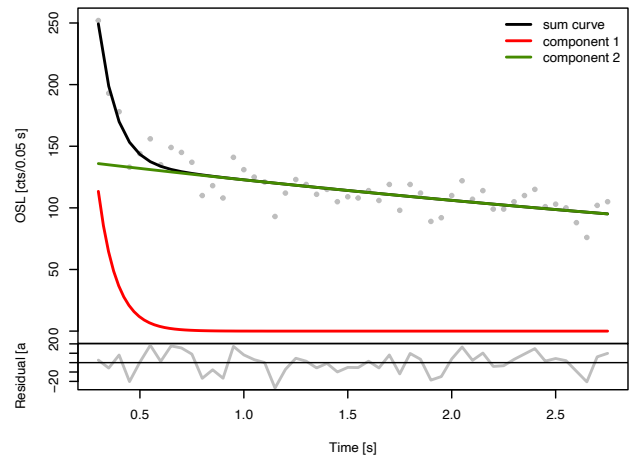
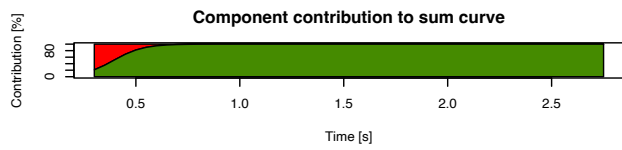
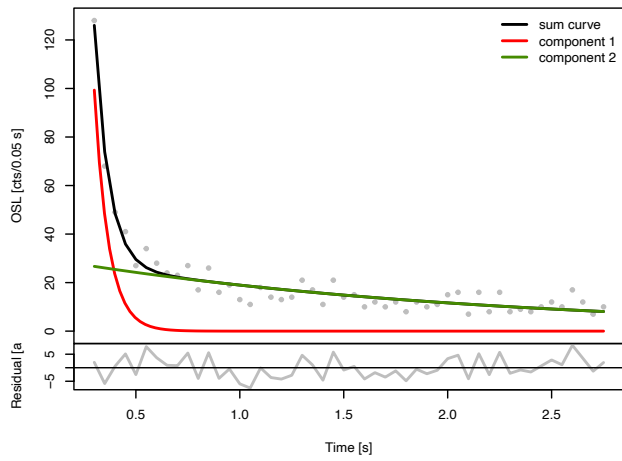
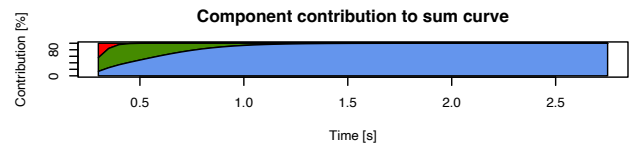
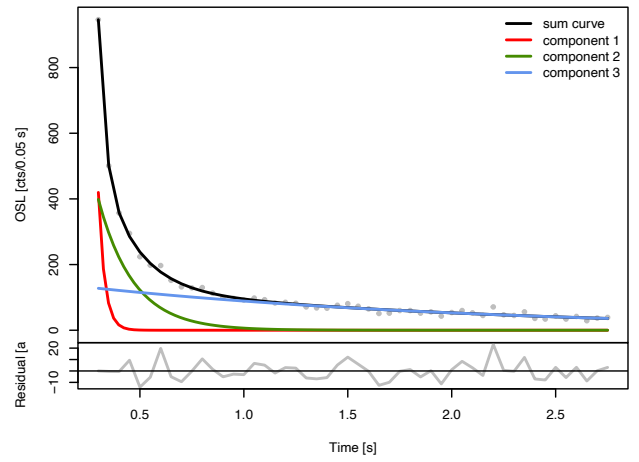
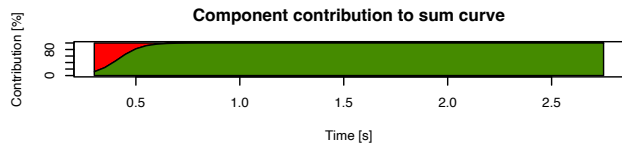
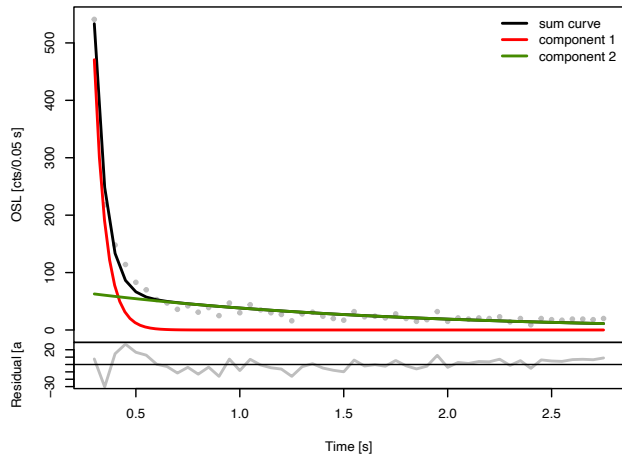


Figure S7. OSL decomposition of four randomly selected signals of sample ZR229.

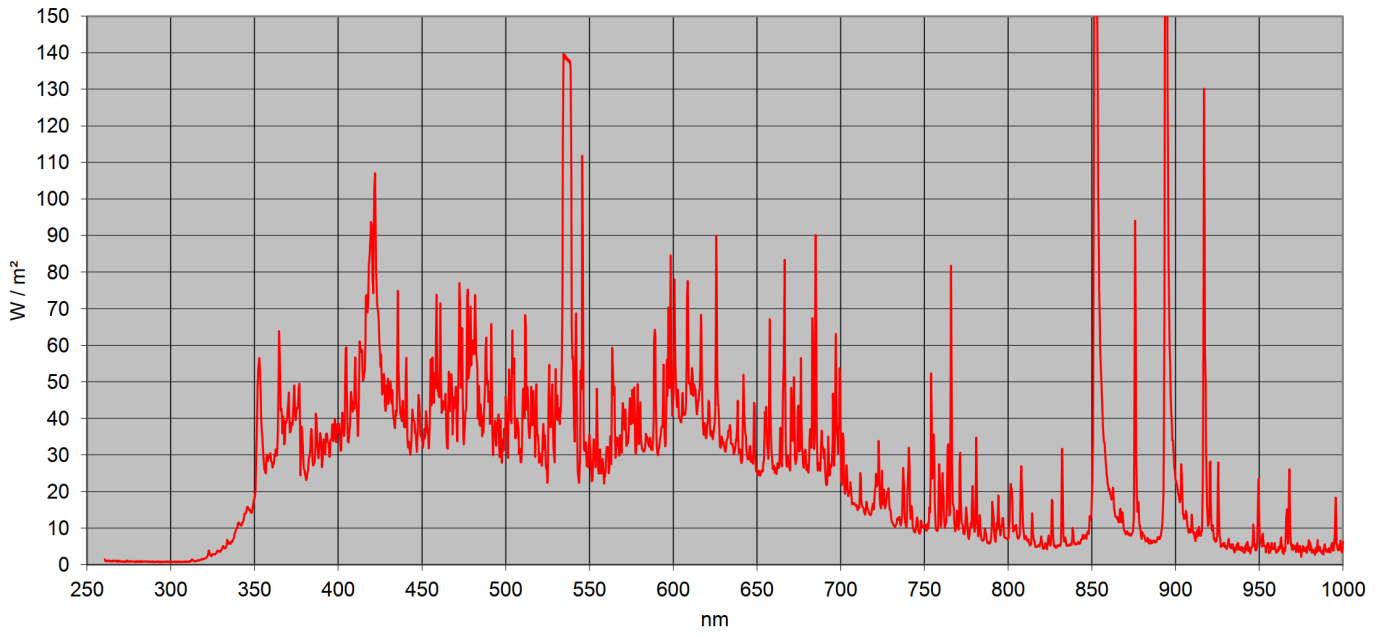


Figure S8. Emission spectrum of the bulb built in the Hönle UVACube 400 used to bleach the zircon samples (data from the manufacturer).